J|A|C|S
ARTICLES
Published on Web 03/09/2002

The Laser-Induced Blue State of Bacteriorhodopsin: Mechanistic and Color Regulatory Roles of Protein−Protein Interactions, Protein−Lipid Interactions, and Metal Ions

Mark B. Masthay,*,† David M. Sammeth,‡ Merritt C. Helvenston,‡ Charles B. Buckman,†,§ Wuyi Li,‡,⊥ Michael J. Cde-Baca,‡ and John T. Kofron†,||

Contribution from the Department of Chemistry, Murray State University, 456 Blackburn Science Building, Murray, Kentucky 42071-3346 and the Department of Chemistry, New Mexico Highlands University, Las Vegas, New Mexico 87701

Received January 17, 2001

Abstract: In this paper we characterize the mechanistic roles of the crystalline purple membrane (PM) lattice, the earliest bacteriorhodopsin (BR) photocycle intermediates, and divalent cations in the conversion of PM to laser-induced blue membrane (LIBM; $\lambda_{max} = 605$ nm) upon irradiation with intense 532 nm pulses by contrasting the photoconversion of PM with that of monomeric BR solubilized in reduced Triton X-100 detergent. Monomeric BR forms a previously unreported *colorless monomer* photoproduct which lacks a chromophore band in the visible region but manifests a new band centered near 360 nm similar to the 360 nm band in LIBM. The 360 nm band in both LIBM and colorless monomer originates from a Schiff base-reduced retinyl chromophore which remains covalently linked to bacterioopsin. Both the PM→LIBM and monomer→colorless monomer photoconversions are mediated by similar biphotonic mechanisms, indicating that the photochemistry is localized within single BR monomers and is not influenced by BR−BR interactions. The excessively large two-photon absorptivities ($\geq 10^6$ cm^4 s molecule^{-1} photon^{-1}) of these photoconversions, the temporal and spectral characteristics of pulses which generate LIBM in high yield, and an action spectrum for the PM→LIBM photoconversion all indicate that the PM→LIBM and Mon→CMon photoconversions are both mediated by a sequential biphotonic mechanism in which I^*_{460} is the intermediate which absorbs the second photon. The purple→blue color change results from subsequent conformational perturbations of the PM lattice which induce the removal of Ca^{2+} and Mg^{2+} ions from the PM surface.

I. Introduction

Since its discovery in 1971,[1] bacteriorhodopsin (BR; see Figure 1) has become one of the most extensively studied of all proteins due to its ready availability, its thermal stability[2−9] and photostability,[10−14] its similarity to vertebrate visual pigments[1,15,16] and other G protein-coupled receptors,[16] and its potential applications in photonic devices.[15,17] BR, which imparts color to the "purple membrane" (PM) of the archaebacterium *Halobacterium salinarium*,[1,15,18,19] is a 248-residue, 26 kDa chromophoric transmembrane protein consisting of seven α-helices oriented around a common center, in which an all-*trans*-retinyl protonated Schiff base chromophore (ATRPSB, see Figure 2) is covalently linked to the protein backbone at the Lys-216 residue.[15,20] Upon absorbing a photon of visible light, ATRPSB isomerizes to the 13-*cis* conformation, leading to a series of global conformational changes in BR which result in the pumping of a proton across the PM, generating a transmembrane proton gradient which is coupled to the generation of ATP under conditions of low oxygen concentration.[15,18]

The PM is isolated as sheets of ∼0.5 μm diameter, each of which contain ∼30 000 BR molecules arranged as a hexagonal

* To whom correspondence should be addressed. Telephone: (270) 762-6540. Fax: (270) 762-6474. E-mail: mark.masthay@murraystate.edu.
† Murray State University.
‡ New Mexico Highlands University.
§ Current Address: Kemlite Corporation, 8500 CW Post Road, Jonesboro, AR 72401.
⊥ Current Address: Accelrys Inc., 9685 Scranton Road, San Diego, CA 92121.
|| Current Address: Qualis Incorporated, 4600 Park Avenue, Des Moines, IA 50321.

(1) Oesterhelt, D.; Stoeckenius, W. *Nature New Biol.* **1971**, *233*, 149−152.
(2) Jackson, M. B.; Sturtevant, J. M. *Biochemistry* **1992**, *17*, 911−915.
(3) Brouillette, C. G.; Muccio, D. D.; Finney, T. K. *Biochemistry* **1987**, *26*, 7431−7438.
(4) Dancsházy, A.; Tokaji, Z.; Dér, A. *FEBS Lett.* **1999**, *450*, 154−157.
(5) Etoh, A.; Etoh, H.; Mitaki, S. *J. Phys. Soc. Jpn.* **1997**, *66*, 975−978.
(6) Cladera, J.; Galisteo, M. L.; Sabes, M.; Mateo, P. L.; Padros, E. *Eur. J. Biochem.* **1992**, *207*, 581−585.
(7) Gao, M.; Boucher, F. *Toxicol. Lett.* **1998**, *100*, 393−396.
(8) Shnyrov, V. L.; Mateo, P. L. *FEBS Lett.* **1993**, *324*, 237−240.
(9) Galisteo, M. L.; Sanchez-Ruiz, J. M. *Eur. Biophys. J.* **1993**, *22*, 25−30.
(10) Lam, E.; Packer, L. *Arch. Biochem. Biophys.* **1983**, *221*, 557−564.
(11) Dencher, N. A.; Heyn, M. P. *Methods Enzymol.* **1982**, *88*, 5−10.
(12) del Río, E.; González-Mañas, J. M.; Gurtubay, J. G.; Goñi, F. M. *Arch. Biochem. Biophys.* **1991**, *291*, 300−306.
(13) Tan, E. H. L.; Birge, R. R. *Biophys. J.* **1996**, *70*, 2385−2395.
(14) Casadio, R.; Stoeckenius, W. *Biochemistry* **1980**, *19*, 3374−3381.
(15) Birge, R. R. *Annu. Rev. Phys. Chem.* **1990**, *41*, 683−733.
(16) Palczewski, K.; Kumasaka, T.; Hori, T.; Behnke, C. A.; Motoshima, H.; Fox, B. A.; Le Trong, I.; Teller, D. C.; Okada, T.; Stenkamp, R. E.; Yamamoto, M.; Miyano, M. *Science* **2000**, *289*, 739−745.
(17) Birge, R. R.; Gillespie, N. B.; Izaguirre, E. W.; Kusnetzow, A.; Lawrence, A. F.; Singh, D.; Song, Q. W.; Schmidt, E.; Stuart, J. A.; Seetharaman, S.; Wise, K. J. *J. Phys. Chem. B* **1999**, *103*, 10746−10766.
(18) Henderson, R. *Annu. Rev. Biophys. Bioeng.* **1977**, *6*, 87−109 and references therein.
(19) Henderson, R.; Unwin, P. N. T. *Nature* **1975**, *257*, 28−32.
(20) Wang, J.; El-Sayed, M. A. *Photochem. Photobiol.* **2001**, *73*, 564−571.

10.1021/ja010116a CCC: $22.00

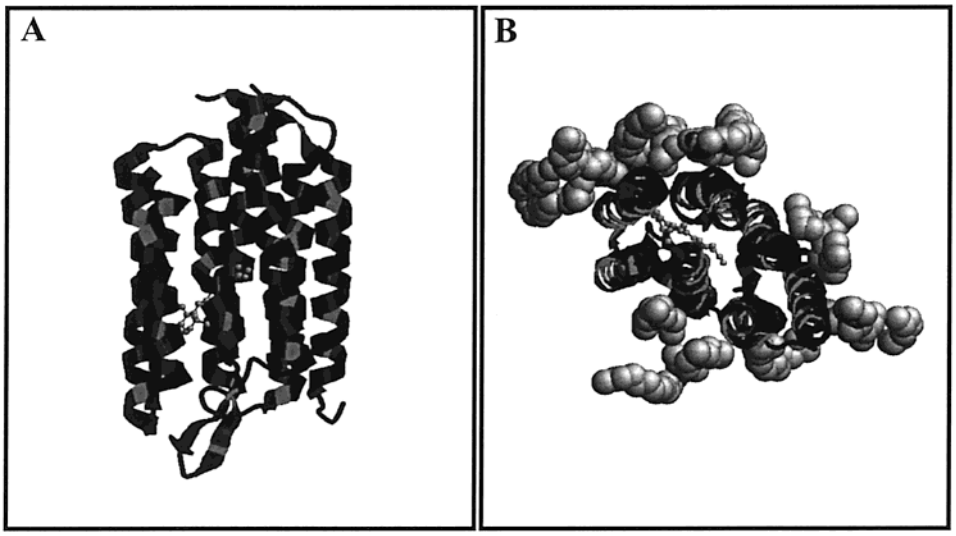

Figure 1. (A) Side view of bacteriorhodopsin (BR), showing its membrane-spanning α-helical structure and the covalently bound retinyl chromophore in the protein interior. (B) Top view of BR, showing the circular arrangement of its seven α-helices, the covalently bound retinyl chromophore in the protein interior, and surrounding purple membrane lipids. Figures correspond to the ground state of the E204Q BR mutant as presented in Luecke, H.; Schobert, B.; Cartailler, J.-P.; Richter, H.-T.; Rosengarth, A.; Needleman, R.; Lanyi, J. K. *J. Mol. Biol.* **2000**, *300*, 1237−1255, the coordinates of which are deposited in the RCSB Protein Data Bank with accession code 1F50.

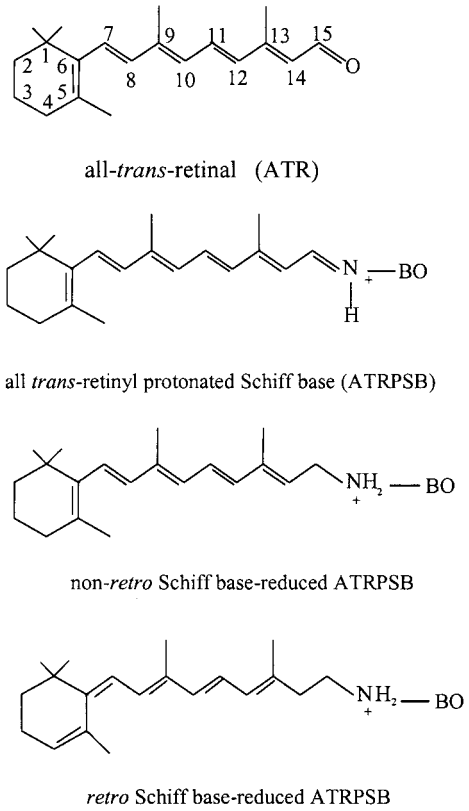

Figure 2. Structures of all-*trans*-retinal (ATR), all-*trans*-retinyl-protonated Schiff base (ATRPSB), non-*retro* Schiff base-reduced-ATRPSB, and *retro* Schiff base-reduced ATRPSB, in which BO represents bacterioopsin, the apoprotein of bacteriorhodopsin. Carbon atom indices are shown for ATR only, but are identical for all species.

lattice of trimers (*p*3 crystallographic point group with 62 Å separating the centers of nearest-neighbor trimers; BR number density ∼150 000 BR molecules μm^{-2}) which spans a lipid bilayer.[18,19,21−23] There are approximately 10 lipid molecules for every BR molecule in PM, of which the bulk (>90% by mass) are saturated.[2,18,19,24−26] BR accounts for 75% of the total mass and 50% of the surface area of the PM, with polar (23%) and nonpolar (2%) lipids accounting for the remaining mass[2,13,18,19,24−26] and surface area.[26]

In contrast to typical metabolically active membranes, which are highly fluid,[26,27] the PM is strikingly rigid, as the PM lattice immobilizes BR both laterally and rotationally.[18,26,28−31] The viscosity of halobacterial membrane lipids (0.36−5 Poise)[29,31,32] is 10^3-10^4 times smaller than that of PM (≥7,000 Poise),[31] indicating that the rigidity of the PM lattice originates primarily from BR−BR interactions.[29,31] This unusual regularity and rigidity suggest that BR−BR and BR−lipid interactions may regulate the function and optical properties of BR in PM. In these regards, it is known that BR−BR and BR−lipid interactions regulate the lifetime of the M_{410} photocycle intermediate,[10,11,33−36] as well as BR photochemistry in both the early (pre-K_{590})[22,23,34,37−53] and later stages of the photocycle. BR−BR and/or BR−lipid interactions also impart photostability[10−14]

(21) Shen, Y.; Safinya, C. R.; Liang, K. S.; Ruppert, A. F.; Rothschild, K. A. *Nature* **1993**, *366*, 48−50 and references therein.
(22) Kriebel, A. N.; Albrecht, A. C. *J. Chem. Phys.* **1976**, *65*, 4675−4583.
(23) Ebrey, T. G.; Becher, B.; Mao, B.; Kilbride, P.; Honig, B. *J. Mol. Biol.* **1977**, *112*, 377−397.
(24) Szundi, I.; Stoeckenius, W. *Biophys. J.* **1989**, *56*, 369−383 and references therein.
(25) Kates, M.; Kushwaha, S. C.; Sprott, G. D. *Methods Enzymol.* **1982**, *88*, 98−111.
(26) Jain, M. K.; Wagner, R. C. *Introduction to Biological Membranes*; John Wiley and Sons: New York, 1980.
(27) Fliesler, S. J.; Anderson, R. E. *Prog. Lipid Res.* **1983**, *22*, 79−131.
(28) Ahl, P. L.; Cone, R. A. *Biophys. J.* **1984**, *45*, 1039−1049.
(29) Korenstein, R.; Hess, B. *FEBS Lett.* **1978**, *89*, 15−20.
(30) Razi Naqvi, K.; Gonzalez-Rodriguez, J.; Cherry, R. J.; Chapman, D. *Nature New Biol.* **1973**, *245*, 249−251.
(31) Sherman, W. V.; Slifkin, M. A.; Caplan, S. R. *Biochim. Biophys. Acta* **1976**, *423*, 238−248.
(32) Lanyi, J. K. *Biochim. Biophys. Acta* **1974**, *356*, 245−256.
(33) Mukhopadhyay, A. K.; Bose, S.; Hendler, R. W. *Biochemistry* **1994**, *33*, 10889−10895.
(34) Shrager, R. I.; Hendler, R. W.; Bose, S. *Eur. J. Biochem.* **1995**, *229*, 589−595.
(35) Lanyi, J. K.; Varo, G. *Isr. J. Chem.* **1995**, *35*, 365−385.
(36) Tokaji, Z. *FEBS Lett.* **1998**, *423*, 343−346.
(37) El-Sayed, M. A. *Acct. Chem. Res.* **1992**, *25*, 279−286 and references therein.
(38) Fitter, J.; Verclas, S. A. W.; Lechner, R. E.; Seelert, H.; Dencher, N. A. *FEBS Lett.* **1998**, *433*, 321−325.
(39) Polland, H. J.; Franz, M. A.; Zinth, W.; Kaiser, W.; Kolling, E.; Oesterhelt, D. *Biophys. J.* **1986**, *49*, 651−662.

and thermal stability[2−9] to BR, since BR in native PM is more resistant to bleaching and denaturation than BR in PM exposed to organic solvents,[54−56] anesthetics,[7] detergents,[10−14,24,57] and elevated temperatures.[2−9,21]

In addition to the roles described above, BR−BR and BR−lipid interactions also contribute to the binding of M^{2+} (M^{2+} = $Ca^{2+}$and Mg^{2+}) and H^+ ions to PM,[1,20,24,56,58−71] which in turn regulates the color, wavelength absorption maximum,[1,10−14,20,24,56,59,62,65,67−75] and proton-pumping capabilities[1,20,24,56,58,62−71,76] of BR, as PM converts to a "cation-free blue membrane" (CFBM) upon the removal of Ca^{2+} and Mg^{2+} ions[24,62−68] and to an "acid blue membrane" (ABM) at pH ≤ 3.5,[1,24,56,62,65,67−71] neither of which pumps protons. The nature and location of the cation binding sites is currently in dispute and is the subject of intense investigation by a number of research groups. The binding sites may consist of pairs of closely coupled carboxylate moieties on the protein surface or in the protein interior,[20,58,62,66] pairs of lipid phosphate and sulfate moieties on the membrane surface,[20,24,77] and combinations of BR COO^- and anionic lipid moieties.[20,24,72,73,77,78] There is also some evidence which suggests that cation binding is entirely nonspecific, with the ions residing in the Gouy−Chapman layer at the membrane surface.[20,24,79,80] Regardless of the nature and origin of cation binding, it is clear that the color of CFBM and ABM is associated with perturbations of the native BR−BR and BR−lipid interactions.

In addition to CFBM and ABM, which are reasonably well understood, a number of research groups have reported a *laser-induced blue membrane* (LIBM) species which results from the irradiation of PM suspensions with high-intensity laser pulses.[81−85] While LIBM bears some similarities to CFBM and ABM, it differs from these species in a number of important ways. The principal objective of the research described below is to characterize the structural and color regulatory roles of BR−BR interactions in LIBM and other blue BR species, as well as their mechanistic roles in the generation of LIBM. LIBM is a particularly good system for characterizing photocooperative BR−BR interactions since the photon fluxes required to generate LIBM are high enough to simultaneously photoexcite two BR monomers within a trimer.[81−85] Secondary objectives of this research include identification of the photointermediate which mediates the generation of LIBM and structural characterization of the retinyl chromophore in LIBM.

In this contribution we describe three novel BR species which we have recently generated[81] from PM, LIBM, and monomeric BR (Mon). We designate these species *colorless monomer* (*CMon*), *monomerized laser-induced blue membrane* (*monomerized LIBM*), and *photolyzed cation-free blue membrane* (*photolyzed CFBM*). These species provide new insights into the roles of BR−BR and BR−lipid interactions and M^{2+} ions in the generation of LIBM, the nature of the photointermediate which mediates the PM→LIBM photoconversion, and the structure of the retinyl chromophore in LIBM, as described below.

II. Experimental Section

A. Sample Preparation. Aqueous PM suspensions were purchased from Biological Components Corporation (Palo Alto, CA) at BR concentrations of $3.8-6.1 \times 10^{-4}$ M and diluted to concentrations of 10^{-6} M < $[BR]_0$ < 3×10^{-5} M in pH = 6.9−7.4 phosphate buffer prior to all experiments unless otherwise specified. Appropriately diluted PM suspensions were placed in standard 1 cm path length cuvettes and light-adapted using light from slide projectors passed through a 475 nm long pass filter (Oriel no. 51290) and a 2 cm path length of aqueous 15% w:v $CuSO_4 \cdot 5H_2O$ solution prior to all sample preparations and experiments. Concentrations and molar extinction coefficients for all species were obtained assuming $\epsilon_{568}^{PM} = 63\,000\ M^{-1}\ cm^{-1}$.

(40) Nuss, M. C.; Zinth, W.; Kaiser, W.; Kölling, E.; Oesterhelt, D. *Chem. Phys. Lett.* **1985**, *117*, 1−7.
(41) Sineschekov, V. A.; Balashov, S. P.; Litvin, F. F. *Biophysics (Engl. Transl. Biofizika)* **1981**, *26*, 986−995.
(42) Gillbro, T.; Sundstrom, V. *Photochem. Photobiol.* **1983**, *37*, 445−455.
(43) Balashov, S. P.; Karneeva, N. V.; Imasheva, E. S.; Litvin, F. F. *Biophysics (Engl. Transl. Biofizika)* **1986**, *31*, 1070−1073.
(44) Balashov, S. P.; Litvin, F. F.; Sineschekov, V. A. In *Physicochemical Biology Reviews*; Skulachev, V. P., Ed.; Harwood Academic Publishers: Chur, Switzerland, 1988; Vol. 8, pp 1−61.
(45) Sineschekov, V. A.; Litvin, F. F. *Biochim. Biophys. Acta* **1977**, *462*, 450−466.
(46) Sharkov, A. V.; Pakulev, A. V.; Chekalin, S. V.; Matveetz, Y. A. *Biochim. Biophys. Acta* **1985**, *808*, 94−102.
(47) Govindjee, R.; Becher, B.; Ebrey, T. G. *Biophys. J.* **1978**, *22*, 67−77.
(48) Wu, S.; El-Sayed, M. A. *Biophys. J.* **1991**, *58*, 190−197.
(49) El-Sayed, M. A.; Lin, C. T.; Mason, W. R. *Proc. Natl. Acad. Sci. U.S.A.* **1989**, *86*, 5376−5379.
(50) El-Sayed, M. A.; Karvaly, B.; Fukumoto, J. M. *Proc. Natl. Acad. Sci. U.S.A.* **1981**, *78*, 7512−7516.
(51) Cassim, J. Y. *Biophys. J.* **1992**, *63*, 1432.
(52) Wu, S.; Awad, E. S.; El-Sayed, M. A. *Biophys. J.* **1991**, *59*, 70−75.
(53) Kataoka, M.; Mihara, K.; Kamikubo, H.; Needleman, R.; Lanyi, J. K.; Tokunaga, F. *FEBS Lett.* **1993**, *333*, 111−113.
(54) Mitaku, S.; Suzuki, K.; Odashima, S.; Ikuta, K.; Suwa, M.; Kukita, F.; Ishikawa, M.; Itoh, H. *Proteins: Struct., Funct., Genet*, **1995**, *22*, 350−362.
(55) Torres, J.; Padros, E. *Biophys. J.* **1995**, *68*, 2049.
(56) Mowery, P. C.; Lozier, R. H.; Chae, Q.; Tseng, Y. W.; Taylor, M.; Stoeckenius, W. *Biochemistry* **1979**, *18*, 4100−4107 and references therein.
(57) Schreckenbach, T.; Walckhoff, B.; Oesterhelt, D. *Eur. J. Biochem.* **1977**, *76*, 499−511.
(58) Yang, D.; El-Sayed, M. A. *Biophys. J.* **1995**, *69*, 2056−2059.
(59) Heyn, M. P.; Dudda, C.; Otto, H.; Seiff, F.; Wallat, I. *Biochemistry* **1989**, *28*, 9166−9172.
(60) Marinetti, M. *Biophys. J.* **1988**, *54*, 197−204 and references therein.
(61) Bose, S.; Mukhopadyay, A. K.; Dracheva, S.; Hendler, R. W. *J. Phys. Chem.* **1997**, *101*, 10584−10587.
(62) Jonas, R.; Ebrey, T. G. *Proc. Natl. Acad. Sci. U.S.A.* **1991**, *88*, 149−153.
(63) Zhang, N. Y.; El-Sayed, M. A. *Biochemistry* **1993**, *32*, 14173−14175.
(64) Tuzi, S.; Yamaguchi, S.; Tanio, M.; Konishi, H.; Inoue, S.; Naito, A.; Needleman, R.; Lanyi, J. K.; Saito, H. *Biophys. J.* **1999**, *76*, 1523−1536 and references therein.
(65) Gerwert, K.; Ganter, U. M.; Siebert, F.; Hess, B. *FEBS Lett.* **1987**, *213*, 39−44.
(66) Stuart, J. A.; Vought, B. W.; Zhang, C. F.; Birge, R. R. *Biospectroscopy* **1995**, *1*, 9−28 and references therein.
(67) Fu, X.; Bressler, S.; Ottolenghi, M.; Eliash, T.; Friedman, N.; Sheves, M. *FEBS Lett.* **1997**, *416*, 167−170.
(68) Kimura, Y.; Ikegami, A.; Stoeckenius, W. *Photochem. Photobiol.* **1984**, *40*, 641−646.
(69) Hu, J. G.; Griffin, R. G.; Herzfeld, J. *J. Am. Chem. Soc.* **1997**, *119*, 9495−9498.
(70) Nasuda-Kouyama, A.; Fukuda, K.; Lio, T.; Kouyama, T. *Biochemistry* **1990**, *19*, 6778−6788.
(71) Hardy, J. P.; Knight, A. E.; Ghiggino, K. P.; Smith, T. A.; Rogers, P. J. *Photochem. Photobiol.* **1984**, *39*, 81−88.
(72) Baribeau, J.; Boucher, F. *Biochim. Biophys. Acta* **1987**, *890*, 275−278.
(73) Padrós, E.; Duñach, M.; Sabés, M. *Biochim. Biophys. Acta* **1984**, *796*, 1−7.
(74) Lugtenburg, J.; Muradin-Szweykowska, M.; Heeremans, C.; Pardoen, J. A.; Harbison, C. S.; Herzfeld, J.; Griffin, R. G.; Smith, S. O.; Mathies, R. A. *J. Am. Chem. Soc.* **1986**, *108*, 3104−3105.
(75) Kamo, N.; Yoshimoto, M.; Kobatake, Y.; Itoh, S. *Biochim. Biophys. Acta* **1987**, *904*, 179−186.
(76) Birge, R. R.; Murray, L. P.; Zidovetzki, R.; Knapp, H. M. *J. Am. Chem. Soc.* **1987**, *109*, 2090−2101.
(77) Roux, M.; Seigneuret, M.; Rigaud, J.-L. *Biochemistry* **1988**, *27*, 7009−7015.
(78) Lanyi, J. K.; Plachy, W. Z.; Kates, M. *Biochemistry* **1974**, *13*, 4914−4920.
(79) Varo, G.; Brown, L. S.; Needleman, L. S.; Lanyi, J. K. *Biophys. J.* **1999**, *76*, 3219−3226.
(80) Szundi, I.; Stoeckenius, W. *Proc. Natl. Acad. Sci. U.S.A.* **1987**, *84*, 3681−3684.
(81) Masthay, M. B.; Buckman, C. B.; Chen, J.; Helvenston, M. C.; Kofron, J. T.; Sammeth, D. M. *Photochem. Photobiol. Special Issue* **1998**, *67S*, 27S-28S.
(82) Govindjee, R.; Balashov, S. P.; Ebrey, T. G. *Biophys. J.* **1990**, *58*, 597−608.
(83) Czege, J.; Reinisch, L. *Photochem. Photobiol.* **1991**, *53*, 659−666.
(84) Chizhov, I. V.; Engelhard, M.; Sharkov, A. V.; Hess, B. In *Structures and Functions of Retinal Proteins*; Rigaud, J. L., Ed.; John Libbey Eurotext, Ltd.: Paris, 1992; pp 171−173.
(85) Balashov, S. P. *Isr. J. Chem.* **1995**, *35*, 415−428.

Laser-Induced Blue Membrane (LIBM). LIBM was prepared by irradiating PM suspensions with 0.6 cm diameter, 8 ns, 532 nm pulses from a Spectra Physics model GCR-11-3 pulsed Nd:YAG laser operating at 10 Hz with typical actinic powers of 6.7 MW cm^{-2} (15 mJ $pulse^{-1}$) until the absorbance maximum of the chromophore band dropped to ~50% of its initial value and the samples appeared blue, with λ_{max} between 579 and 590 nm.

BR Monomer (Mon). Mon was prepared by solubilizing PM in reduced Triton X-100 detergent (reduced-TX; Sigma-Aldrich, used as purchased). We used reduced-TX instead of normal TX to facilitate spectroscopic analysis in the UV region. In our initial PM solubilization step we added 1 mL of a 1% v:v (~1% w:w) solution of reduced-TX in pH = 6.9 phosphate buffer to 1 mL of a 2.5 mg BR/mL aqueous suspension of PM. Our procedure was otherwise identical to the method of Dencher and Heyn.[11] The resulting suspensions—which were purple and nonturbid—consisted of BR monomers incorporated into reduced-TX micelles (critical micelle concentration = 0.015% v:v)[86] with a 4:1 w:w reduced-TX:BR ratio and a 0.5% v:v detergent:buffer ratio. These concentrated Mon suspensions were diluted with appropriate volumes of buffer or 0.5% v:v detergent:buffer solutions prior to irradiation.

Colorless BR Monomer (CMon). CMon was prepared by irradiating suspensions of Mon with 6.7 MW cm^{-2}, 532 nm pulses until the absorbance maximum of the chromophore band dropped to <50% of its initial value and the samples were faint purple or colorless to the eye. To prepare our **monomerized laser-induced blue membrane (monomerized LIBM)** suspensions, we monomerized 100% LIBM suspensions using the procedures described above.

Cation-Free Blue Membrane (CFBM). CFBM was prepared by passing PM suspensions (unbuffered to avoid adding Na^+ and K^+ ions to the suspensions) through a 15 mm × 20 cm gravity column packed with 9−10 g of Bio-Rad AG50W-X8 biotechnological grade 100−200 mesh hydrogen form cation-exchange resin at pH = 5 according to the technique of Kimura, et al.[68] The column slurry was rinsed with deionized water at pH = 5.9 until the pH of the water leaving the column was equal to that entering the column. 1−2 drops of [BR] = 3.8×10^{-4} M suspensions of PM were placed at the top of the columns; ~1 mL aliquots of CFBM were collected at the bottom of the columns. We subsequently generated **photolyzed cation-free blue membrane (photolyzed CFBM)** by irradiating CFBM suspensions with 6.7 MW cm^{-2}, 532 nm pulses until A_{601} decreased by ~50%.

Monomerized Cation-Free Blue Membrane (Monomerized CFBM). This compound was prepared by converting PM to CFBM and subsequently monomerizing the resultant CFBM. Upon centrifugation, the monomerized CFBM separated into two layers: a nonturbid, light purple layer on the top (λ_{max} = 560 nm) similar to normal Mon and a turbid, dark purple layer (λ_{max} = 556 nm) on the bottom. The spectroscopic properties of monomerized CFBM given below are based on spectra of the top layer, which had a more distinct chromophore band.

B. Sample Spectra and Composition. UV−visible absorption spectra were obtained with a Hewlett-Packard model 8451 UV−visible spectrophotometer. Two fluorescence emission (λ_{exc} = 280 and 360 nm) and two fluorescence excitation spectra (λ_{emis} = 330 and 490 nm) spectra were obtained for each species using Shimadzu model RF-5301 PC or SPEX Fluorolog-II spectrofluorometers. All spectra were obtained with $[BR]_0 = 1-4 \times 10^{-5}$ M samples placed in 1 cm path length absorption or fluorescence cuvettes.[87]

We calculated the % photoconversion of reactants R (PM, Mon, or CFBM) to photoproducts P (LIBM, CMon, or photolyzed CFBM) by monitoring decreases in the absorbance at 532 nm according to

$$\%\text{photoconversion} = \%\text{P} = 100 \times \frac{A^R_{532} - A^t_{532}}{A^R_{532} - \text{A}^P_{532}} \qquad (1)$$

in which A^R_{532} and A^t_{532} are the absorbance values after 0 and t seconds of laser irradiation, respectively, and A^P_{532} is the absorbance after R has been completely converted to P. A^P_{532} was assumed to be constant and equal to $0.49A^{PM}_{532}$, $0.20A^{Mon}_{532}$, and $0.62A^{CFBM}_{532}$ for the PM→LIBM, Mon→CMon, and CFBM→photolyzed CFBM photoconversions, respectively.[87]

C. Actinic Power Dependence. To specify the role of BR−BR interactions in the generation of LIBM, we contrasted the actinic power dependence of the Mon→CMon and PM→LIBM photoconversions. As the power dependence for the PM→LIBM photoconversion was previously reported as quadratic,[84] our principal objective was to characterize the power dependence of the Mon→CMon photoconversion.

We performed three separate sets of power dependence studies of the Mon→CMon photoconversion (two with high [$A^{initial}_{532} \approx 1.0$] and one with low [$A^{initial}_{532} \approx 0.1$] initial absorbance). For brevity we report only the results of our low-absorbance studies. All data points used in the low-absorbance studies corresponded to ~20% drops in absorbance. Actinic powers in the low absorbance studies ranged from 0.67 to 7.1 MW cm^{-2}, with total actinic doses ranging from 51.3 to 6.4 J, respectively.

D. Action Spectrum. To characterize the intermediate which absorbs the second photon in the PM→LIBM photoconversion, we obtained an action spectrum ($\Phi^{PM\rightarrow LIBM}_{\lambda}$ vs λ) with ~7.6 MW cm^{-2} (3 mJ, 2 ns, 0.3 cm^2 beam cross section) pulses over wavelengths ranging from 400 to 580 nm using a Spectra Physics GCR-270-MOPO-730 Nd:YAG-pumped optical parametric oscillator system. The $A^{initial}_{532}$ values ranged from 0.721 to 0.766, with $100 \times (\Delta A_{532}/A^{initial}_{532})$ ranging from 0.52 to 16.02%.[87]

III. Results

A. Spectroscopic Characterization of BR Species. A glossary and schematic description of the various BR species described below is given in Figure 3. The absorption spectra of PM, LIBM, Mon, CMon, monomerized LIBM, CFBM, and photolyzed CFBM are given below. Their fluorescence excitation and emission spectra are summarized in the Supporting Information.[87]

PM. Consistent with reports in the literature,[82] our light-adapted PM samples were characterized by a chromophore band with λ^{PM}_{max} = 568 nm, $W^{PM}_{1/2}$ = 3700 cm^{-1}, ϵ^{PM}_{568} = 63 000 M^{-1} cm^{-1}, and ϵ^{PM}_{532} = 49 000 M^{-1} cm^{-1}, and a Trp band with λ_{max} = 280 nm and ϵ_{280} = 140 000 M^{-1} cm^{-1} (see Figure 4).

LIBM. Consistent with reports in the literature,[82−85] our aqueous PM suspensions (λ_{max} = 568 nm) turned blue upon irradiation with intense 532 nm pulses, with a concomitant bathochromic shift of the chromophore band from to λ_{max} = 580 nm ($\Delta E_{max} = -365$ cm^{-1}) and an ~50% decrease in the absorbance maximum upon converting 91% of the PM to LIBM (see Figure 4). The Trp band of PM was photostable, as A_{280} decreased by only 5% upon converting PM to LIBM.[82,83] Isosbestic regions formed near 420 and 615 nm upon converting PM to LIBM. The 420 nm region resulted from a reduced chromophore photoproduct we designate P^{LIBM}_{360}, which was characterized by a structured band with peaks at 340, 360, and 380 nm which was ~$^2/_3$ as intense as the chromophore band of PM.[82−84] The 615 nm region originated from one or more bathoproducts which we collectively designate P^{LIBM}_{605}. Both the

(86) Tiller, G. E.; Mueller, T. J.; Docktor, M. E.; Struve, W. G. *Anal. Biochem.* **1984**, *141*, 262−266.

(87) See Supporting Information, which contain further details regarding (1) deconvolution of the spectra of pure LIBM and CMon from those of PM + LIBM and Mon + CMon mixtures and the physical origin of the small initial Mon-to-CMon bathochromic shift, (2) fluorescence spectra, (3) ΔA_{400} calculations, (4) quantum yields, (5) the PM-to-LIBM action spectrum, and (6) details of our titrations of CFBM and LIBM with metal cations.

Relationships between PM, LIBM and monomerized LIBM

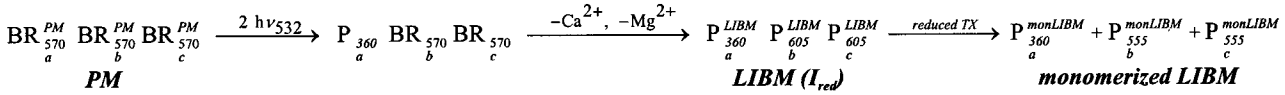

Relationships between PM, Mon, and CMon

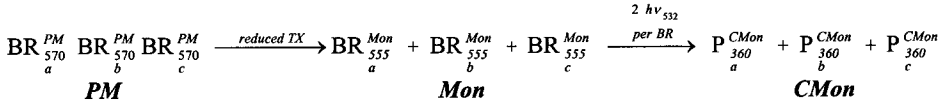

Relationships between PM, CFBM, photolyzed CFBM, and monomerized CFBM

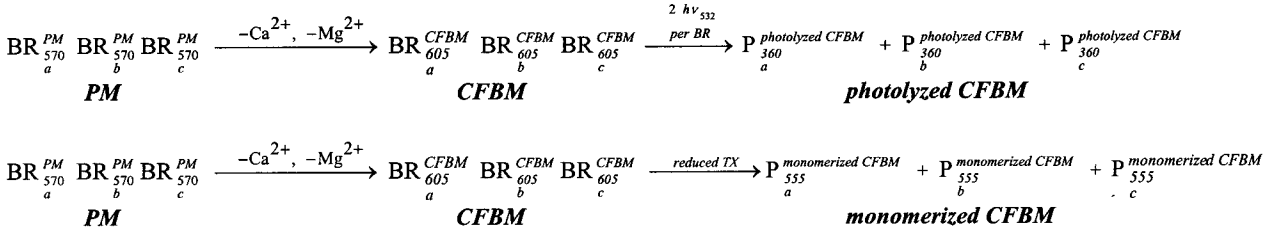

Figure 3. Relationships between purple membrane (PM), laser-induced blue membrane (LIBM), BR monomers (Mon) solubilized in reduced Triton X-100 (reduced TX) detergent, colorless monomer (CMon), monomerized LIBM, cation-free blue membrane (CFBM), photolyzed CFBM, and monomerized CFBM. For brevity we show only the I_{red} component of LIBM. LIBM is actually a 50% I_{red} + 50% II_{red} mixture, in which $II_{red} = P^{LIBM}_{360a}\ p^{LIBM}_{360b}\ P^{LIBM}_{605c}$ (see text).

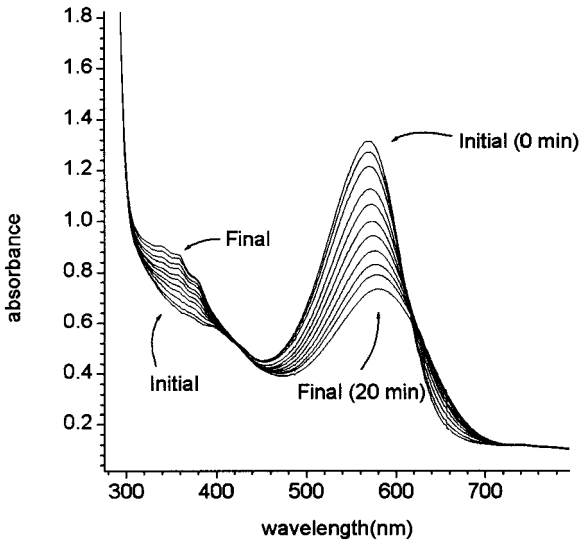

Figure 4. Generation of 91% LIBM from 100% PM with 6.7 MW cm^{-2}, 532 nm pulses. Spectra were obtained after 0 (initial), 2, 4, 6, 8, 10, 12, 14, 16, 18, and 20 (final) min of irradiation with a frequency-doubled Nd:YAG laser operating at 10 Hz (12 000 pulses total).

bathochromic shift and the 615 nm isosbestic region were reversible upon the addition of monovalent or divalent metal cations, but the original intensity was only partially restored.[83] The spectrum of pure LIBM, obtained by deconvoluting the spectrum of pure LIBM from that of PM + LIBM mixtures using techniques detailed in the Supporting Information,[87] has a chromophore band with $\lambda_{max} = 605$ nm, $\epsilon^{LIBM}_{605} = 31\,000\ M^{-1}\ cm^{-1}$, $\epsilon^{LIBM}_{532} = 24\,000\ M^{-1}\ cm^{-1}$, and $W^{LIBM}_{1/2} = 4300\ cm^{-1}$.[82-84]

Mon. Our light-adapted Mon samples were characterized by a chromophore band with $\lambda^{Mon}_{max} = 555$ nm, $W^{Mon}_{1/2} = 3700\ cm^{-1}$, $\epsilon^{Mon}_{555} = 42\,000\ M^{-1}\ cm^{-1}$, and $\epsilon^{Mon}_{532} = 36\,000\ M^{-1}\ cm^{-1}$, and a Trp band essentially identical to that of PM, in reasonable agreement with the literature (see Figure 5).[10-14]

CMon. Upon irradiation with 532 nm pulses, our Mon suspensions progressively became colorless without turning blue, consistent with the small 555→560 nm ($\Delta E_{max} = -161\ cm^{-1}$) bathochromic shift in the λ_{max} observed upon converting Mon to 55% CMon (see Figure 5). Upon continued irradiation the chromophore band disappeared and the suspensions became colorless. The Trp band was effectively photostable. Isosbestic regions formed near 425 and 620 nm. The 425 nm region resulted from a P^{Mon}_{360} photoproduct which was characterized by an unstructured band with $\lambda_{max} = 365$ nm and was ~45% as intense as the chromophore band of Mon. The 620 nm region was 5 nm wide (50% narrower than the 10 nm wide 615 nm PM→LIBM isosbestic region) and was not reversible upon the addition of metal cations. On close inspection, most of the spectra were approximately parallel and did not intersect in this region, suggesting that bathoproducts are not present in CMon.[87]

Our ***monomerized LIBM*** samples were purple in appearance, with chromophore band λ_{max} and $W_{1/2}$ values identical to those of Mon. However, the chromophore band was only one-third to two-thirds as intense as that of Mon (see Figure 6). Upon adding reduced-TX to LIBM, the three peaks of the P^{LIBM}_{360} band converged into a single broad band which peaked at 338 nm

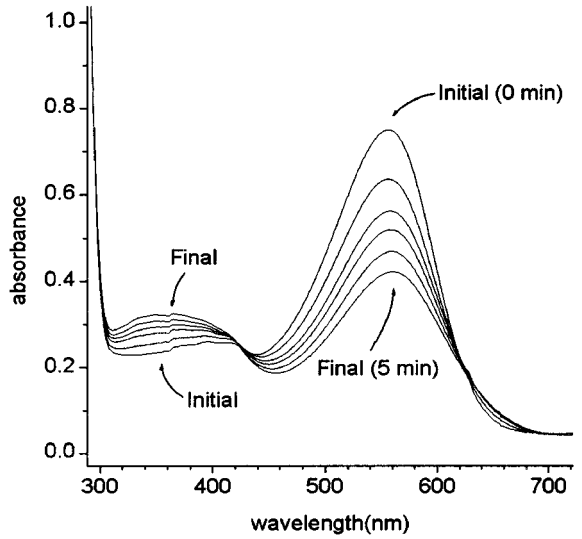

Figure 5. Generation of 55% CMon from 100% Mon with 6.7 MW cm^{-2}, 532 nm pulses. Spectra were obtained after 0 (initial), 1, 2, 3, 4, and 5 (final) min of irradiation with a frequency-doubled Nd:YAG laser operating at 10 Hz (3000 pulses total).

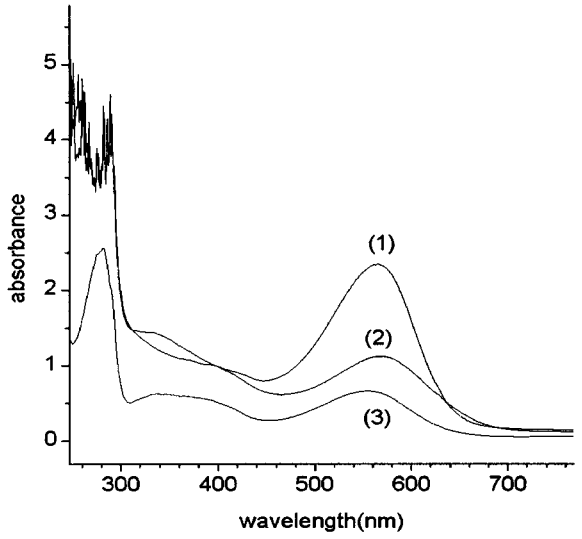

Figure 6. Spectra of (1) light-adapted PM, (2) 100% LIBM generated by exposing PM to 18 min of irradiation with 6.7 MW cm^{-2}, 532 nm pulses from a frequency-doubled Nd:YAG laser operating at 10 Hz (10 800 pulses total), and (3) monomerized LIBM generated from 100% LIBM using a standard monomerization procedure (see Experimental Section).

with an intensity roughly equal to that of the chromophore band of monomerized LIBM. The Trp band was essentially identical to that of Mon.

CFBM and Monomerized CFBM. Consistent with reports in the literature,[68,88] our CFBM samples were characterized by a chromophore band with $\lambda_{max}^{CFBM} = 601$ nm and $W_{1/2}^{CFBM} = 4700$ cm^{-1}, a shoulder at ~400 nm, and a Trp band similar to that of PM (see Figure 7). Monomerized CFBM, with $\lambda_{max}^{monomerizedCFBM} = 560$ nm and $W_{1/2}^{monomerizedCFBM} = 3900$ cm^{-1}, was spectroscopically similar but not identical to monomerized LIBM.

Photolyzed CFBM. Upon converting CFBM to 83% photolyzed CFBM, the λ_{max} of the chromophore band shifted hypsochromically from 601 to 580 nm, the ϵ_{max} decreased by

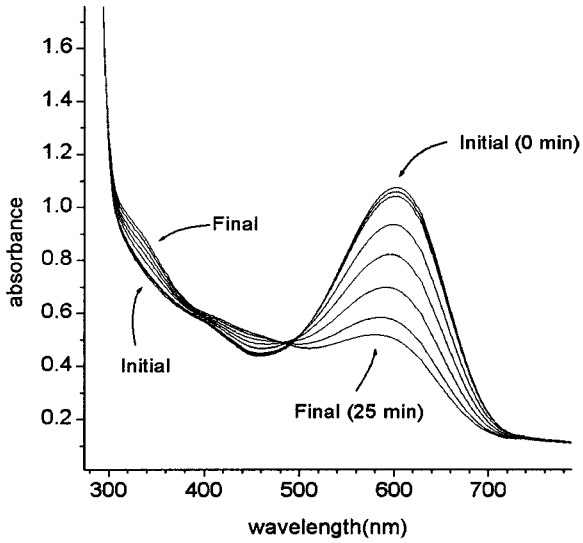

Figure 7. Generation of 83% photolyzed CFBM from 100% CFBM with 6.7 MW cm^{-2}, 532 nm pulses. Spectra were obtained after 0 (initial), 1, 2, 7, 12, 17, 22, and 25 (final) min of irradiation with a frequency-doubled Nd:YAG laser operating at 10 Hz (15 000 pulses total).

~50%, and the band broadened somewhat (see Figure 7). There was a slight and unstructured increase in absorbance in the 300−500 nm region which we attribute to a $P_{360}^{photolyzedCFBM}$ photoproduct.[57,82,83,89,90] An isosbestic region appeared at ~487 nm, but no isosbestic region occurred near 620 nm. The Trp band was essentially photostable.

B. Quantum Yields. Upon exposing ~2 mL aliquots of optically thin ($A_{532}^{initial} = 0.2$) samples of Mon and PM to 100 laser pulses (4.8 MW cm^{-2}, 532 nm), the *actinically active absorbances* $A_{532}^{Monchrom}$ and $A_{532}^{PMchrom}$—which we define as the total absorbance minus light-scattering contributions (the latter of which accounted for 20 and 30% of the initial total absorbance of Mon and PM at 532 nm)—decreased by 62 and 53%, respectively, corresponding to quantum yields of $\Phi_{532}^{Mon\rightarrow CMon} = 0.70\%$ pulse$^{-1} = 7.4 \times 10^{-4}$ molecule photon^{-1} and $\Phi_{532}^{PM\rightarrow LIBM} = 0.43\%$ pulse$^{-1} = 5.2 \times 10^{-4}$ molecule photon^{-1}. The quantum yields were based on actinically active rather than total absorbance because scattered light is not intense enough to induce nonlinear effects.[87]

C. Nonlinear Character of the Mon→CMon and PM→LIBM Photoconversions. 1. Actinic Power Dependence. The accuracy of photochemically based actinic power dependence studies is enhanced by the use of low-absorbance samples since the actinic intensities—and hence the probility of multiphoton absorption—are approximately constant over the entire optical path length and since normalized absorbance changes $\Delta A/A$ are approximately independent of concentration in low-absorbance samples.[84,87,91,92] Hence, although we consistently obtained nonlinear power dependence for both low- and high-

(88) Chang, C. H.; Chen, J. G.; Govindjee, R.; Ebrey, T. G. *Proc. Natl. Acad. Sci. U.S.A.* **1985**, *82*, 396−400.
(89) Birge, R. R.; Bocian, D. F.; Hubbard, L. M. *J. Am. Chem. Soc.* **1982**, *104*, 1196−1207.
(90) Druckmann, S.; Renthal, R.; Ottolenghi, M.; Stoeckenius, W. *Photochem. Photobiol.* **1984**, *40*, 647−665.
(91) Angelov, D. A.; Kryukov, P. G.; Letokhov, V. S.; Nikogosyan, D. N.; Oraevskii, A. A. *Sov. J. Quantum Electron.* **1980**, *10*, 746−753.
(92) Masthay, M. B.; Helvenston, M. C. Characterization of actinic power dependence in systems which undergo irreversible multiphoton-induced photochemistry. In *Program and Abstracts*; Gomer, C. H., Scientific Program Chair, Ed.; American Society for Photobiology: Chicago, IL, 2001; pp 28.

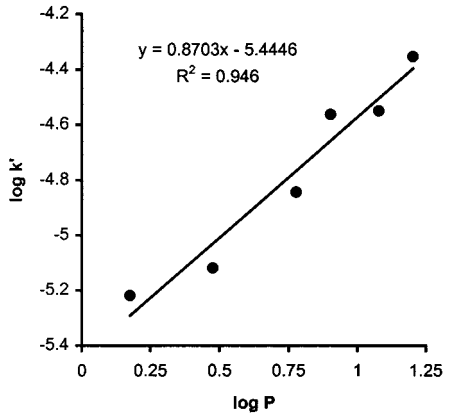

Figure 8. Linear-least squares best-fit plot (correlation coefficient $R^2 = 0.946$) of log k' vs log $P_{actinic}$, in which k' is the rate constant normalized to total actinic dosage for the Mon→CMon photoconversion (see eq 7 in text). Since slopes of log k' vs log $P_{actinic}$ are equal to $n - 1$ for nth order processes, the observed slope of 0.87 indicates that the rate of the Mon→CMon photoconversion is proportional to $P_{actinic}^{1.87}$. Hence the Mon→CMon photoconversion is mediated by a consecutive biphotonic or two-photon absorption mechanism.

absorbance samples, we report only the results of our low-absorbance studies.

We determined the power dependence of the Mon→CMon photoconversion using the method of initial rates[84,87,91] assuming a rate R which is first-order in the actinically active absorbance $A_{555}^{\text{Monchrom}}$ at 555 nm and nth order in the actinic power $P_{actinic}$:

$$R = -\frac{1}{10}\frac{\Delta A_{555}^{Monchrom}}{\Delta t} = -kA_{555}^{average}\,P_{actinic}^{n} \qquad (2)$$

In eq 2, $A_{555}^{average}$ is the average actinically active absorbance over an irradiation interval of Δt seconds, k is a rate constant with units of mJ^{-n} $pulse^{n-1}$, and the factor of 10 originates from the 10 Hz repetition rate of the laser. To obtain n we normalized eq 2 to $A_{555}^{average}$ and the total actinic dosage $E_{tot} = 10\Delta t\ P_{actinic}$ to yield eq 3[84,91,92]

$$\frac{R}{E_{tot}A_{555}^{average}} = -\frac{\Delta A_{555}}{10\Delta t P_{actinic}A_{555}^{average}} = kP_{actinic}^{\,n-1} = k' \qquad (3)$$

in which k' (units = mJ^{-1}) was equal to the slope of $R/E_{tot}A_{555}^{average}$ vs Δt for the earliest 20% of the photoconversion process. A plot of log k' vs log $P_{actinic}$ yielded a slope of $n - 1 = 0.87$ for the Mon→CMon photoconversion (see Figure 8).[84,91,92] Hence, R is proportional to $P_{actinic}^{1.87}$, indicating that the Mon→CMon photoconversion is mediated by either a two-photon process[93] or a sequential biphotonic[94] process. In similar fashion, we found the PM→LIBM power dependence to range from $n = 1.5-1.8$, consistent with reports in the literature.[82,84,87]

2. Two-Photon Absorptivities. On the basis of conventional two-photon theory,[93,95] which assumes that a molecule simultaneously absorbs two photons, the average number of BR molecules per pulse which underwent two-photon excitation under the actinic power conditions we used to obtain the PM→LIBM and Mon→CMon and quantum yields is

$$N_{532}^{BR**} = \frac{1}{2\sqrt{2}}N_{h\nu}P_0C_{BR}^{average}\frac{z_{02}}{\pi w_{02}^{\,2}}\delta_{532}^{BR} \qquad (4)$$

in which $N_{h\nu} = 2.94 \times 10^{16}$ photon $pulse^{-1}$ is the number of photons in an 11 mJ pulse, $P_0 = N/(1.06447\tau_{pulse}) = 3.45 \times 10^{24}$ photon sec^{-1} is the number of photons per second at peak intensity, $C_{BR}^{\text{average}PM\rightarrow LIBM} = 1.9 \times 10^{15}$ molecules cm^{-3} and $C_{BR}^{averageMon\rightarrow CMon} = 2.3 \times 10^{15}$ molecules cm^{-3} are the average actinically active concentrations for the $A_{532}^{initial} \approx 0.20$ (PM) → $A_{532}^{final} \approx 0.15$ (PM + LIBM) and $A_{532}^{initial} \approx 0.20$ (Mon) → $A_{532}^{final} \approx 0.10$ (Mon + CMon) solutions used in our studies, the path length $z_{02} = 1$ cm, the beam radius w_{02} is equal to 0.3 cm, and δ_{532}^{BR} is the two-photon absorptivity of BR for 532 nm photons. Multiplying all of the factors above, eq 4 reduces to

$$N_{532}^{BR**inPM} = (2.4 \times 10^{56}\ \text{GM}^{-1}\ \text{pulse}^{-1}\ \text{molecule}) \times \delta_{532}^{BRinPM} \qquad (5a)$$

and

$$N_{532}^{BR**inMon} = (2.9 \times 10^{56}\ \text{GM}^{-1}\ \text{pulse}^{-1}\ \text{molecule}) \times \delta_{532}^{BRinMon} \qquad (5b)$$

for the PM→LIBM and Mon→CMon photoconversions, respectively, in which 1 GM = 1 Goeppert−Mayer = 1×10^{-50} cm^4 s $photon^{-1}$ $molecule^{-1}$ is the standard unit of two-photon absorptivity.[93,95] Assuming that the PM→LIBM and Mon→CMon photoconversions are mediated by simultaneous two-photon absorption and that each BR molecule which absorbs two 532 nm photons converts to photoproduct, we may equate the percentages of doubly excited molecules in the beam path with the % $pulse^{-1}$ quantum yields:

$$\%(\text{BR}^{**}\text{ in PM}) = 100 \times (N_{532}^{BR**inPM}/N_{beampath}^{BRinPM}) = \Phi_{532}^{PM\rightarrow LIBM} \qquad (6a)$$

$$\%(\text{BR}^{**}\text{ in Mon}) = 100 \times (N_{532}^{BR**inMon}/N_{beampath}^{BRinMon}) = \Phi_{532}^{Mon\rightarrow CMon} \qquad (6b)$$

Combining eqs 5a and 6a and eqs 5b and 6b, substituting $N_{beampath}^{BRinPM} = 5.7 \times 10^{14}$ molecules and $N_{beampath}^{BRinMon} = 6.9 \times 10^{14}$ molecules, and solving for δ_{532}^{BRinPM} and $\delta_{532}^{BRinMon}$ yields

$$\delta_{532}^{BRinPM} = (2.4 \times 10^{-44}\ \text{GM pulse})\ \Phi_{532}^{PM\rightarrow LIBM} \qquad (7a)$$

and

$$\delta_{532}^{BRinMon} = (2.4 \times 10^{-44}\ \text{GM pulse})\ \Phi_{532}^{Mon\rightarrow CMon} \qquad (7b)$$

Substituting the quantum yields reported above into eqs 7 yields $\delta_{532}^{BRinPM} = 1.0 \times 10^6$ GM and $\delta_{532}^{BRinMon} = 1.7 \times 10^6$ GM. These values are exceptionally large (see Figure 9).[93,95−97]

D. Titrations of CFBM and LIBM with Ca^{2+} and Na^+. To determine if metal cations are removed from PM during the PM→LIBM photoconversion, we contrasted the effects of added Na^+ and Ca^{2+} ions on the spectra of CFBM and LIBM by

(93) Birge, R. R. *One-photon and two-photon excitation spectroscopy*; Kliger, D. S., Ed.; Academic Press: New York, 1983; pp 109−175.
(94) Lachish, U.; Schafferman, A.; Stein, G. *J. Chem. Phys.* **1976**, *64*, 4205−4211.
(95) Birge, R. R.; Zhang, C.-F. *J. Chem. Phys.* **1990**, *92*, 7178−7195.
(96) Geactinov, N. E.; Breton, J. *Exciton annihilation and other nonlinear high-intensity excitation effects*; Alfano, R. R., Ed.; Academic: New York, 1982; pp 157−191.
(97) Arsenault, R.; Denariez-Roberge, M. M. *Chem. Phys. Lett.* **1976**, *63*, 84−87.

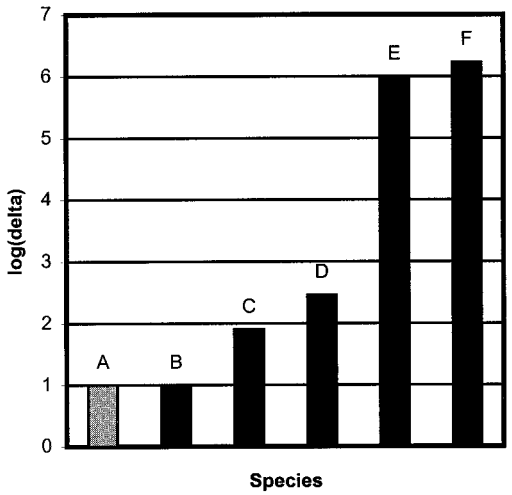

Figure 9. Base 10 logarithm of the two-photon absorptivities δ_λ (units: GM = 1×10^{-50} cm^4 s photon^{-1} molecule^{-1}; wavelength λ in nm) for various species, illustrating the highly atypical behavior of bacteriorhodopsin (BR). A = δ for typical virtual state-mediated two-photon transitions (shown in gray to represent the *range* of typical two-photon absorptivities); B = estimated δ_{532} of tryptophan; C = estimated δ_{532} of BR assuming all two-photon absorptivity originates from its 8 tryptophan residues; (D) largest reported two-photon absorptivity for inhomogeneously broadened transitions reported to date (290 GM; see ref 95); (E) experimental δ_{532} of BR in PM as calculated using eq 7a; (F) experimental δ_{532} of BR solubilized in Triton X-100 as calculated using eq 7b.

titrating samples of CFBM and LIBM with 0.010 M NaCl and 0.00010 M $CaCl_2$ (see Table 1 and details provided in the Supporting Information[87]). Consistent with reports in the literature,[24,68,77] CFBM turned purple ~100 times more efficiently on a per mol basis upon titration with Ca^{2+} ($\Delta\lambda_{max}$ = −36 nm upon adding 11 mol of Ca^{2+} per mol of BR) than upon titration with Na^+ ($\Delta\lambda_{max}$ = −35 nm upon adding 1100 mol of Na^+ per mol of BR). In contrast, the λ_{max} shifted to the blue by ≤2 nm and the samples failed to turn purple when ~80% LIBM suspensions were titrated with NaCl and with $CaCl_2$.

To determine if laser pulses lower the specificity of the binding sites for divalent cations we performed another set of titrations to characterize the relative efficiencies with which Na^+ and Ca^{2+} ions induce hypsochromic shifts in LIBM by using titrants of sufficient concentration (3.0 M $CaCl_2$ and 3.0 M NaCl) to induce blue→purple transitions. We limited our analysis to the first four 25 μL aliquots in these high concentration titrations, as determination of the λ_{max} became difficult upon further addition of 3.0 M $CaCl_2$ due to significant increases in light scattering. In contrast to CFBM, the λ_{max} of LIBM shifted hypsochromically only 2−3 times more efficiently upon titration with Ca^{2+} ($\Delta\lambda_{max}$ = −8 nm upon adding 14 000 mol of Ca^{2+} per mol of BR) than with Na^+ ($\Delta\lambda_{max}$ = −3 nm upon adding 14 000 mol of Na^+ per mol of BR).

IV. Discussion

A. Mechanistic Implications of Quadratic Actinic Power Dependence and Large Biphotonic Absorptivities. As demonstrated above, the rates at which LIBM and CMon are generated depend quadratically on actinic power, indicating that the photochemical event which initiates the PM→LIBM and Mon→CMon photoconversions involves the absorption of two photons. Short-lived virtual intermediate states,[84] Trp residues,[82] photocooperative multi-exciton species,[83] the excited singlet state BR*,[82,84,85] the BR photocycle intermediates J_{625} and K_{590},[82−85] iso-BR[41,43,44,82,85,98,99] and pseudo-BR[41−44,82,85,98−100] could all potentially act as intermediates in the PM→LIBM photoconversion. As demonstrated below, our data indicate that the principal intermediate is the I^*_{460} (post-Franck−Condon) component of BR*.[101]

Table 1. Cation-Induced Hypsochromic Shifts of the Chromophore Bands of CFBM and LIBM[a]

Effects of Na^+ and Ca^{2+} on λ_{max} of CFBM

	$\left\lvert \frac{\Delta\lambda_{max}(nm)}{\mu mole\ titrant} \right\rvert$	$\frac{\Delta\lambda_{max}^{Ca^{2+}}}{\Delta\lambda_{max}^{Na^+}}$	$\frac{moles\ titrant}{moles\ BR}$
NaCl	3.5		1,100
		$\frac{350}{3.5} = 100$	
$CaCl_2$	350		11

B. Effects of Na^+ and Ca^{2+} on λ_{max} of ~20% PM : ~80% LIBM Mixtures

	$\left\lvert \frac{\Delta\lambda_{max}(nm)}{\mu mole\ titrant} \right\rvert$	$\frac{\Delta\lambda_{max}^{Ca^{2+}}}{\Delta\lambda_{max}^{Na^+}}$	$\frac{moles\ titrant}{moles\ BR}$
NaCl	0.01		14,000
		$\frac{0.027}{0.01} = 2.7$	
$CaCl_2$	0.027		14,000

C. Effects of Na^+ and Ca^{2+} on λ_{max} of CFBM and LIBM Contrasted

$$\left\lvert \frac{\Delta\lambda_{max}^{CFBM}}{\mu mole\ Na^+} \right\rvert \Big/ \left\lvert \frac{\Delta\lambda_{max}^{LIBM}}{\mu mole\ Na^+} \right\rvert = \frac{3.5}{0.01} = 350$$

$$\left\lvert \frac{\Delta\lambda_{max}^{CFBM}}{\mu mole\ Ca^{2+}} \right\rvert \Big/ \left\lvert \frac{\Delta\lambda_{max}^{LIBM}}{\mu mole\ Ca^{2+}} \right\rvert = \frac{350}{0.027} = 13{,}000$$

[a] Our results indicate that (A) Ca^{2+} hypsochromically shifts λ_{max}^{CFBM} ~100 times more efficiently than Na^+, (B) λ_{max}^{LIBM} is ~40 times less sensitive to Ca^{2+} (as compared to Na^+) than λ_{max}^{CFBM}, suggesting that irradiation of PM with intense 532 nm pulses reduces the selectivity of the cation binding sites for divalent cations, and (C) the Na^+- and Ca^{2+}-induced hypsochromic shifts of λ_{max}^{LIBM} are smaller than those of λ_{max}^{CFBM} by more than 2 and 4 orders of magnitude, respectively, suggesting that the binding efficiencies of both Na^+ and Ca^{2+} are reduced significantly upon irradiation with intense 532 nm pulses. See text for additional details.

Temporal and Spectral Characteristics of the Intermediate in the PM→LIBM and Mon→CMon Photoconversions. According to current models[37,39,40,101−106] the BR photocycle is

(98) Balashov, S. P.; Karneeva, N. V.; Litvin, F. F.; Sineschekov, V. A.; Ovchinikov, Y. A., Ed.; In *Retinal Proteins*; VNU Science Press: Utrecht, 1987; pp 505−517.
(99) Sineschekov, V. A.; Balashov, S. P.; Litvin, F. F. *Biophysics (Engl. Transl. Biofizika)* **1984**, *29*, 1082−1088.
(100) Gillbro, T.; Kriebel, A. N.; Wild, U. P. *FEBS Lett.* **1977**, *78*, 57−60.
(101) Zhong, Q.; Ruhman, S.; Ottolenghi, M.; Sheves, M.; Friedman, N.; Atkinson, G. H.; Delaney, J. K. *J. Am. Chem. Soc.* **1996**, *118*, 12828−12829.
(102) Atkinson, G. H.; Ujj, L.; Zhou, Y. *J. Phys. Chem A* **2000**, *104*, 4130−4139.
(103) Haran, G.; Wynne, K.; Xie, A.; He, Q.; Chance, M.; Hochstrasser, R. M. *Chem. Phys. Lett.* **1996**, *261*, 389−395.
(104) Hasson, K. C.; Gai, F.; Anfinrud, P. A. *Proc. Natl. Acad. Sci. U.S.A.* **1996**, *93*, 15124−15129.
(105) Gai, F.; Hasson, K. C.; McDonald, J. C.; Anfinrud, P. A. *Science* **1998**, *279*, 1886−1891 and references therein.

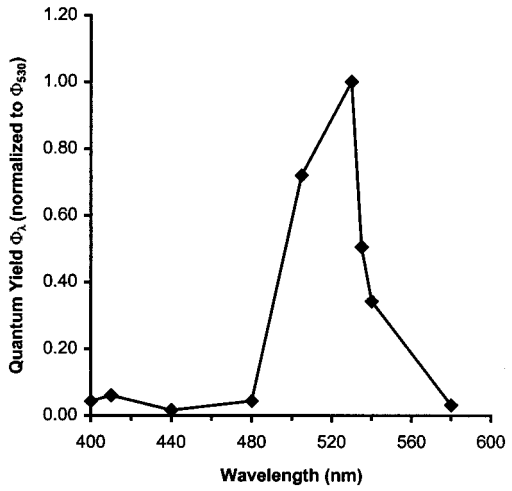

Figure 10. Normalized action spectrum for the PM→LIBM photoconversion obtained with 7.6 MW cm^{-2} (3 mJ, 2 ns, 0.2 cm^2) pulses from an optical parametric oscillator pumped with the third harmonic from a pulsed Nd:YAG laser. Quantum yields $\Phi_\lambda^{PM\rightarrow LIBM}$ are normalized to $\Phi_{530}^{PM\rightarrow LIBM}$.

best represented as

$$BR_{570} \xrightarrow{h\nu,\ <50\ fs} BR^*_{fast} \xrightarrow{>200\ fs} BR^*_{slow} = I^*_{460} \xrightarrow{500\ fs} J_{625} \xrightarrow{>2\ ps} K_{590} \xrightarrow{>1\ \mu s} \text{later intermediates} \rightarrow BR_{570}.$$

In principle, then, it should be possible to identify the intermediate which mediates the PM→LIBM photoconversion by matching the temporal and spectral characteristics of actinic pulses to those of the intermediate. Regarding the temporal requirements, it is significant that Chizhov, et al.[84] were able to generate LIBM with 10 ns pulses and 30 ps pulses, but not with 200 fs pulses, indicating that the intermediate which absorbs the second photon must be generated with a rise time 200 fs $< \tau_{rise} <$ 30 ps following the absorption of the first photon.[107]

The spectral characteristics of the intermediate may be inferred from the PM→LIBM action spectrum, which peaks near 530 nm, drops to ~50% of maximum near 500 and 535 nm, and falls nearly to baseline at 480 and 580 nm (see Figure 10).[87] Since $\Phi_\lambda^{PM\rightarrow LIBM}$ is proportional to $\epsilon_\lambda^{BR\rightarrow Int} \times \epsilon_\lambda^{Int\rightarrow Int^*}$, in which Int and Int* designate the intermediate state before and after it has absorbed the second photon, the action spectrum should be intense when both $\epsilon_\lambda^{BR\rightarrow Int}$ and $\epsilon_\lambda^{Int\rightarrow Int^*}$ are large and weak when either of these extinction coefficients are small. Our action spectrum thus indicates that both $\epsilon_\lambda^{BR\rightarrow Int}$ and $\epsilon_\lambda^{Int\rightarrow Int^*}$ are reasonably large between 500 and 540 nm and that one or both of these extinction coefficients must approach zero near 480 and 580 nm, where $\Phi_\lambda^{PM\rightarrow LIBM}$ approaches the baseline.

Short-lived Virtual State Intermediates Do Not Mediate the PM→LIBM and Mon→CMon Photoconversions. Our experimental values for δ_{532}^{BRinPM} and $\delta_{532}^{BRinMon}$ equal or exceed 10^6 GM, more than 3 orders of magnitude larger than the largest two-photon absorptivity reported for inhomogeneously broadened two-photon transitions mediated by short-lived ($\tau \approx 10^{-15}$ s) virtual intermediate states[95,108] and more than 5 orders of magnitude larger than the $\delta \approx 1-10$ GM values typical of two-photon processes mediated by virtual states[93,95] (see Figure 9). Our δ_{532}^{BRinPM} and $\delta_{532}^{BRinMon}$ values thus appear to require long-lived (>100 fs) intermediates, and are consistent with the studies of Chizhov et al., who estimated the lifetime of the PM→LIBM intermediate to be 1.7 ps.[84] We thus conclude that the PM→LIBM and Mon→CMon photoconversions are not mediated by virtual state intermediates.

Tryptophan Residues Do Not Mediate the PM→LIBM and Mon→CMon Photoconversions. Noting that the absorbance at 280 nm decreases slightly (3−4%) during the PM→LIBM photoconversion, Govindjee, et. al. suggested that Trp residues might play a direct role in this process.[82] This suggestion appears reasonable, since Trp residues could conceivably mediate the reduction of ATRPSB by donating electrons to water or hydronium ions to yield aqueous electrons or hydrogen atoms after absorbing two 532 nm photons. We nevertheless conclude that Trp does not mediate the PM→LIBM and Mon→CMon photoconversions, for three reasons.

First, our two-photon absorptivities are much too large to originate from the eight Trp residues in BR since our two-photon cross sections require that δ_{532}^{BRinPM} and $\delta_{532}^{BRinMon} = 1.2 \times 10^5$ GM and that $\delta_{532}^{TrpinPM}$ and $1/8\ \delta_{532}^{BRinPM} = 1/8\ \delta_{532}^{BRinMon} = 2.1 \times 10^5$ GM. These δ_{532}^{Trp} values are not only exceptionally large in general[93,95−97,109,110] but are $1.0-1.7 \times 10^5$ times larger than the approximate theoretical value of $\delta_{532}^{Trp} \approx \delta_{532}^{Indole} \approx 10$ GM (see Figure 9).[109,110]

Second, the 3−4% decrease in absorbance at 280 nm[82,83] which occurs during the PM→LIBM, Mon→CMon and CFBM→photolyzed CFBM photoconversions is 7−10 times smaller than the >30% drop which occurs at the chromophore band absorption maxima, indicating that the Trp residues are effectively photostable. Such stability appears inconsistent with the photooxidation of Trp,[94,111] since $Trp^{\bullet+}$ and related species would be expected to degrade efficiently via subsequent reactions with other amino acid residues in BR, PM lipids, water, and O_2.[111]

Third, Govindjee, et al. found the PM→LIBM photoconversion to be more efficient at pH = 9.7 than at neutral or acidic pH.[82] These results also argue against a Trp-mediated photoreduction of ATRPSB since such a process should occur more efficiently under low pH conditions via the reaction of aqueous electrons with H_3O^+ to produce $H^\bullet$.[90]

Govindjee, et. al. note that at least two Trp residues are close

(106) Gai, F.; McDonald, J. D.; Anfinrud, P. A. *J. Am. Chem. Soc.* **1997**, *119*, 6201−6202.

(107) Chizhov, et. al. generated LIBM with 10 ns, 532 nm pulses, with 10 ns, 610 nm pulses, and with 30 ps, 610 nm pulses, but failed to generate LIBM with 200 fs, 615 nm pulses. Their results were consistent with our action spectrum, however, since they found the yield of LIBM to be significantly higher with 10 ns, 532 nm pulses than with 10 ns, 610 nm pulses. Professor Benno Hess. Private Communication.

(108) Chlorophyll *a* in diethyl ether has a two-photon absorptivity of $\delta \approx 10^7$ GM upon excitation with a pulsed ruby laser (see Arsenault, R., Denariez-Roberge, M. M. *Chem. Phys. Lett.* **1976**, *40*, 84−87, and ref 96 and references therein). These authors ascribed the large δ and value to "resonance phenomena" since the 694.3 nm ruby line overlaps with the intense S_1 absorption band of chlorophyll *a*. The lifetime of the S_1 state of chlorophyll *a* is 15.2 ns, indicating that the large δ value—like that of BR—originates from a sequential biphotonic process which is not mediated by a virtual intermediate state.

(109) Professor P. R. Callis. Private communication.

(110) The two-photon absorptivity of indole is observed experimentally to be roughly 10 times that of benzene and toluene according to Anderson, B. E.; Jones, R. D.; Rehms, A. A.; Ilich P.; Callis, P. R. *Chem. Phys. Lett.* **1985**, *125*, 106−11, Rehms, A. A.; Callis, P. R. *Chem. Phys. Lett.* **1987**, *140*, 83−89, and Callis, P. R. *Chem. Phys. Lett.* **1984**, *107*, 125−130. The *maximum* two-photon absorptivity of benzene is between 0.1 and 1.0 GM at its two-photon λ_{max} of ~6.6 eV = 187 nm, which corresponds energetically to the absorption of two 374 nm photons (see Ziegler, L. D.; Hudson, B. S. *Chem. Phys. Lett.* **1980**, *71*, 113−116); it is less at 266 nm, which corresponds energetically to the absorption of two 532 nm photons. See also Birge, R. R. *Acc. Chem. Res.* **1986**, *19*, 138−146.

(111) Creed, D. *Photochem. Photobiol.* **1984**, *4*, 537−562 and references therein.

to the ATRPSB chromophore and that the small decrease in A_{280} could be due to changes in interactions between these residues and the reduced chromophore.[82] We believe this suggestion is likely to be correct, but note in addition that reduction of the chromophore could also directly contribute to the decrease in A_{280} if $\epsilon_{280}^{reduced-ATRPSB} < \epsilon_{280}^{ATRPSB}$.

Multi-Exciton Intermediates Do Not Mediate the PM→LIBM and Mon→CMon Photoconversions. A *biphotonic two monomer* mechanism, in which two closely associated monomers each simultaneously absorb a single photon to yield a trimeric BR_{570a}^{*} BR_{570b}^{*} BR_{570c}^{*} species which converts to LIBM has been proposed.[83] Our results indicate that the PM→LIBM and Mon→CMon photoconversions are mediated by a common mechanism since both processes manifest quadratic power dependence and have similar quantum yields and since both LIBM and CMon contain non-*retro* Schiff base-reduced chromophores (see below). Since individual Triton X-100 micelles typically contain only a single BR molecule,[112] the fact that $\Phi_{532}^{Mon\rightarrow CMon}$ is slightly larger than $\Phi_{532}^{PM\rightarrow LIBM}$ unequivocally indicates that the photoreduction step in the PM→LIBM photoconversion is mediated by a process in which a single BR monomer absorbs two photons, as $\Phi_{532}^{PM\rightarrow LIBM}$ would exceed $\Phi_{532}^{Mon\rightarrow CMon}$ if multi-exciton states were required. We thus conclude that *the Mon→CMon and PM→LIBM photoconversions are both mediated by a biphotonic one monomer process in which individual BR monomers absorb two photons.*

J_{625}, K_{590}, iso-BR, and pseudo-BR Play Minor Roles (At Most) in the PM→LIBM and Mon→CMon Photoconversions. A *biphotonic one monomer-via-photocycle intermediate* mechanism, in which a single monomer absorbs a photon and is converted to a photocycle intermediate Int = J_{625}, K_{590} iso-BR, or pseudo-BR, which subsequently absorbs the second photon leading to an Int_a^* BR_b^{570} BR_c^{570} species which converts to LIBM, has also been proposed.[82−85] While J_{625} (τ_{rise} = 500 fs; τ_{decay} = 3 ps)[101,102] and K_{590} (τ_{rise} = 3 ps;[37,39,40,84,95,113] τ_{decay} = 2 μs in both PM[40,95,113,114] and Mon[40,114]), iso-BR ($\tau_{rise} \geq$ 3 ps; $\tau_{decay} \geq$ 7 ps),[82,85] and pseudo-BR ($\tau_{rise} \geq$ 3 ps; $\tau_{decay} \geq$ 70 ps)[82,85] all satisfy the temporal requirements for the PM→LIBM intermediate, none of these species has an absorption spectrum consistent with our PM→LIBM action spectrum. J_{625} does not absorb between 500 and 540 nm,[102] and hence is precluded as the intermediate, since our action spectrum is intense in this region. K_{590} is bathochromically shifted with respect to BR_{570}[115] and thus also appears to be precluded as the principal intermediate, since the action spectrum would peak at wavelengths longer than 570 nm in photoconversion mediated exclusively by K_{590}. Furthermore, because the absorption spectra of iso-BR[41,43,44,82,85,98,99] and pseudo-BR[41−44,82,85,98−100] are similar to that of BR, the PM→LIBM action spectrum would be similar to the absorption spectrum of PM if the PM→LIBM photoconversion were mediated by either of these species.

I_{460}^{*} is the Principal Intermediate in the PM→LIBM and Mon→CMon Photoconversions. A *biphotonic one monomer-via-*I_{460}^{*} mechanism

$$PM = \underset{a}{BR_{570}}\ \underset{b}{BR_{570}}\ \underset{c}{BR_{570}} \xrightarrow{h\nu_{532}} \underset{a}{I_{460}^{*}}\ \underset{b}{BR_{570}}\ \underset{c}{BR_{570}} \xrightarrow{h\nu_{532}}$$

$$\underset{a}{I_{460}^{**}}\ \underset{b}{BR_{570}}\ \underset{c}{BR_{570}} \rightarrow \underset{a}{P_{360}}\ \underset{b}{P_{605}}\ \underset{c}{P_{605}} = LIBM$$

has also been proposed,[82−85] in which a single monomer absorbs a photon and converts to I_{460}^{*}, which subsequently absorbs a second photon and converts to LIBM. *We believe this to be the principal mechanism by which the PM→LIBM photoconversion is mediated* for several reasons. First, the temporal characteristics of I_{460}^{*} ($\tau_{rise} \geq$ 100−200 fs; τ_{decay} = 500 fs)[37,39,101,103−105,115] match those required for the intermediate in the PM→LIBM photoconversion. Second, our action spectrum indicates that $\Phi_{\lambda}^{PM\rightarrow LIBM}$ is large at wavelengths ranging between 490 and 530 nm (where $\epsilon_{\lambda}^{BR_{570}\rightarrow I_{460}^{*}}$ and $\epsilon_{\lambda}^{I_{460}^{*}\rightarrow I_{460}^{**}}$ are both reasonably large)[39,104−106,117] and that $\Phi_{\lambda}^{PM\rightarrow LIBM}\rightarrow$0 near 480 nm (where $\epsilon_{\lambda}^{Br_{570}\rightarrow I_{460}^{*}}$ is small) and decreases monotonically at $\lambda >$ 540 nm (where $\epsilon_{\lambda}^{I_{460}^{*}\rightarrow I_{460}^{**}}\rightarrow$0).[39,87,102,104−106,117] Third, because I_{460}^{*} is a resonantly accessed eigenstate of BR with a lifetime much greater than that of typical virtual state intermediates, it is not precluded as an intermediate by our large two-photon cross sections.[93,95−97] Fourth, given the profound difference in the viscosities of PM (≥7000 poise)[31] and reduced-TX (2.4 Poise), it is reasonable to expect photochemical processes which induce conformational changes in BR to be more efficient in Mon than in PM.[38] However, the fact that $\Phi_{532}^{Mon\rightarrow CMon}$ and $\Phi_{532}^{PM\rightarrow LIBM}$ are of the same order of magnitude indicates that the Mon→CMon and PM→LIBM photoconversions are mediated by a mechanism in which the second photon is absorbed before changes in BR conformation occur, and hence is more consistent with fast intermediates such as I_{460}^{*} than with slower intermediates such as K_{590}.[37−40,101,105,116,118] Fifth, while we are not aware of any reports in which BR* or J_{625} in BR monomers have been characterized, the similarities between the post-K_{590} portions of the PM and Mon photocycles[10,11] and the rapid localization of photoexcitation energy in the absorbing monomer in PM trimers[37,39,42−45] suggest that Mon should have an excited singlet state similar to I_{460}^{*} in PM.

B. Spectroscopic Properties of BR Species: Implications Regarding the Structure of LIBM and CMon. Czege and Reinisch[83] suggest that LIBM consists of a Poisson distribution of BR trimers in which the chromophores of zero (PM = BR_{570a}^{PM} BR_{570b}^{PM} BR_{570c}^{PM}), one (I_{red} = P_{360a}^{LIBM} BR_{605b}^{LIBM}

(112) Reynolds, J. A.; Stoeckenius, W. *Proc. Natl. Acad. Sci. U.S.A.* **1977**, *74*, 2803−2804.
(113) Bazhenov, V.; Schmidt, P.; Atkinson, G. H. *Biophys. J.* **1992**, *61*, 1630−1637.
(114) Milder, S. J.; Thorgeirsson, T. E.; Miercke, L. J. W.; Stroud, R. M.; Kliger, D. S. *Biochemistry* **1991**, *30*, 1751−1761.
(115) Kulcsár, Á.; Saltiel, J.; Zimányi, L. *J. Am. Chem. Soc.* **2001**, *123*, 3332−3341.
(116) Song, L.; El-Sayed, M. A. *J. Am. Chem. Soc.* **1998**, *120*, 8889−8890.
(117) The $I_{460}^{*}\rightarrow I_{460}^{**}$ (i.e., $S_1\rightarrow S_n$) absorption spectrum indicated by our action spectrum is in close agreement with reported experimental $S_1\rightarrow S_n$ absorption spectra of BR (see refs 39, 102, and 104−106). It also agrees reasonably well with theoretical $S_1\rightarrow S_n$ absorption spectra calculated using semiempirical molecular orbital methods (see Dinur, U.; Honig, B.; Ottolenghi, M. In *Developments in Biophysical Research*; Borsellino, A., et. al., Eds.; Plenum: New York, 1980; pp 209−221 and Birge, R.; Findsen, L. A.; Pierce, B. M. *J. Am. Chem. Soc.* **1987**, *109*, 5041−5043). The experimental and theoretical $S_1\rightarrow S_n$ absorption spectra are more intense in the 400−500 nm region than in the $\lambda >$ 500 nm region, and are thus consistent with a PM→LIBM action spectrum (proportional to $\epsilon^{BR_{570}\rightarrow I_{460}^{*}} \times \epsilon_{\lambda}^{I_{460}^{*}\rightarrow I_{460}^{**}}$; see text) peaking between 500 and 550 nm, in agreement with our results. Our action spectrum thus indicates that the PM→LIBM and Mon→CMon photoconversions are mediated by high lying S_n states of BR (i.e., $I_{460}^{**} = S_n$ with $n > 2$), and that S_2 (which may be responsible for the recently observed $S_1\rightarrow S_n$ absorbance in the 700−900 nm region; see refs 103−106) plays a significantly smaller role—if any—in these photoconversions.
(118) Aharoni, A.; Weiner, L.; Ottolenghi, M.; Sheves, M. *J. Am. Chem. Soc.* **2001**, *123*, 6612−6616.

BR^{LIBM}_{605c}), two ($II_{red} = P^{LIBM}_{360a}\ BR^{LIBM}_{360b}\ BR^{LIBM}_{605c}$), or three ($III_{red} = P^{LIBM}_{360a}\ BR^{LIBM}_{360b}\ BR^{LIBM}_{360c}$) monomers are reduced. In this model, P^{LIBM}_{360} originates from the BR monomer(s) within a trimer which contain reduced chromophores; P^{LIBM}_{605} originates from the remaining unreduced monomer(s) within the same trimer. The precise nature of the P^{LIBM}_{360} and P^{LIBM}_{605} chromophores has not been specified to date. As discussed below, our studies provide more definitive insights into the structures of the P^{LIBM}_{360} and P^{LIBM}_{605} chromophores than previous studies,[82−84] as well as providing an assessment of the accuracy of the model of Czege and Reinisch.[83]

The Nature of the P_{360} Photoproducts: $\mathbf{P^{LIBM}_{360}}$. Although the λ_{max} of the chromophore band in LIBM is similar to those of CFBM and ABM, the absorption spectrum of LIBM differs from those of CFBM and ABM in two notable ways. First, the chromophore band in LIBM is roughly half as intense as those of PM,[82] CFBM,[68] and ABM.[1,56,71,119] Second, LIBM contains a P^{LIBM}_{360} photoproduct (absent in PM, CFBM, and ABM) which has a structured absorption spectrum with peaks at ~340, ~360, and ~380 nm.

The absorption spectra of retinoids are typically broad and unstructured due to inhomogeneous broadening originating from torsional rotations of the β-ionylidene ring around the C_6-C_7 single bond. In contrast, the spectra of retinoids in which ring torsions are hindered by a $C_6=C_7$ double bond (as occurs in *retro*-retinoids)[57,87,89] or by steric constraints imposed on ring torsions around the C_6-C_7 single bond within the chromophore binding site of BR[57,71,87,89,90,120] (as occurs in borohydride-reduced PM[57,87,89,120] and radiolytically reduced PM,[90] in both of which the C=N bond has been reduced to C−N) manifest vibronic structure. The similarities of the absorption spectrum of P^{LIBM}_{360} to those of various *retro* retinoids,[87,89,121,122] borohydride-reduced PM, and radiolytically reduced PM, in combination with the fluorescence spectrum of LIBM and the spectral properties of P^{CMon}_{360} and $P^{monomerizedLIBM}_{360}$ (see below), lead us to conclude that P^{LIBM}_{360} *originates from BR containing nonretro Schiff base-reduced ATRPSB containing 5 C=C bonds which remains covalently bound to the apoprotein, and that the vibronic structure of* P^{LIBM}_{360} *originates from steric constraints imposed by the chromophore binding site which hinder ring torsions.*

LIBM has a fluorescence excitation spectrum ($\lambda_{emis} = 490$ nm) similar to its absorption spectrum, and a broad emission band centered at 466 nm ($\lambda_{exc} = 360$ nm). P^{LIBM}_{360} originates from changes in ATRPSB and not from changes in the apoprotein, since P^{LIBM}_{360} does not form in PM which has been bleached with hydroxylamine prior to laser irradiation. Because emission is always red-shifted with respect to absorption, the 466 nm emission band cannot originate from P^{LIBM}_{605}, indicating that the 466 nm band originates exclusively from P^{LIBM}_{360} and that P^{LIBM}_{360} and P^{LIBM}_{605} are chemically distinct species.[82] We also observed a weak 466 nm emission band when we excited LIBM with 280 nm light, indicating that Trp residues transfer energy to the P^{LIBM}_{360} chromophore and hence that the P^{LIBM}_{360} chromophore remains localized in the binding site.[87]

We conclude that the P^{LIBM}_{360} chromophore has five double bonds since the 466 nm emission band of LIBM is similar to the emission bands of pulse-radiolyzed PM[87,90] and the non-*retro* species all-*trans*-retinol,[87,121] axerophtene,[87,121] and 1,3,5,7,9-decapentaene,[87,123] each of which has 5 C=C bonds, and since the emission maxima of *retro* and non-*retro*-retinoids with 6 double bonds occur at significantly longer wavelengths ($\lambda^{emis}_{max} > 510$ nm) than that of LIBM.[87,121]

$\mathbf{P^{CMon}_{360}}$ and $\mathbf{P^{monomerizedLIBM}_{360}}$. Aside from their lack of vibronic structure, the absorption spectra of P^{CMon}_{360} and $P^{monomerizedLIBM}_{360}$ are similar to that of P^{LIBM}_{360}, as are their fluorescence spectra. We attribute the lack of vibronic structure in the spectra of P^{CMon}_{360} and $P^{monomerizedLIBM}_{360}$ to detergent-induced relaxation of steric constraints on ring torsions, in analogy with the loss of vibronic structure observed upon adding detergents to borohydride-reduced PM.[57] Our specra thus indicate that both CMon and monomerized LIBM contain covalently bound, non-*retro* Schiff base-reduced ATRPSB chromophores with five C=C bonds. They further indicate that the vibronic structure of P^{LIBM}_{360} originates from C_6-C_7 torsional constraints imposed by the chromophore binding site, since the spectrum of $P^{monomerizedLIBM}_{360}$ would manifest vibronic structure if LIBM contained a *retro* chromophore.[87]

CMon lacks a chromophore band in the visible region,[124] whereas monomerized LIBM has a visible chromophore band with λ_{max} identical to but intensity roughly half that of Mon. Hence, 100% and ~50% of the chromophores are reduced in CMon and monomerized LIBM, respectively. The intensity of the chromophore band in monomerized LIBM thus indicates that both LIBM and monomerized LIBM contain an ~50:50 mixture of native and reduced chromophores, which is consistent with an ~50:50 mixture of I_{red} and II_{red}.[83] The similarities between P^{CMon}_{360} and P^{LIBM}_{360} are particularly significant, as − in agreement with our actinic power dependence studies − they indicate that *the generation of* P^{LIBM}_{360} *is not mediated by BR−BR interactions, but rather originates from photochemistry localized entirely within individual BR molecules.*

$\mathbf{P^{photolyzedCFBM}_{360}}$. While the changes in the absorption spectrum observed during the generation of photolyzed CFBM are not identical to those observed in the PM→LIBM and Mon→CMon photoconversions, an increase in absorbance in the 300−400 nm region similar to those observed during the

(119) Moore, T. A.; Edgerton, M. E.; Parr, G.; Greenwood, C.; Perham, R. N. *Biochem. J.* **1978**, *171*, 469−476.
(120) Peters, J.; Peters, R.; Stoeckenius, W. *FEBS Lett.* **1976**, *61*, 128−134.
(121) Christensen, R. L.; Kohler, B. E. *Photochem. Photobiol.* **1973**, *18*, 293−301.
(122) Das, K. K.; Barua, A. B.; Siddhanta, N. N. *Curr. Sci.* **1969**, *38*, 363−364.-
(123) D'Amico, K. L.; Manos, C.; Christensen, R. L. *J. Am. Chem. Soc.* **1979**, 1777−1782.
(124) Although BR solubilized in detergents is more susceptible to "photobleaching" (i.e., the light-induced separation of the retinyl chromophore from the apoprotein; see ref 13) than BR in native PM (see refs 10−14, 23, and 57) and—like "photobleached" BR—CMon lacks the native purple color of BR, we are confident that the chromophore remains covalently bound to the apoprotein in CMon since (i) the absorption spectrum of P^{CMon}_{360} is markedly flatter and less intense than that of photobleached BR (see refs 13 and 87), (ii) the increase in absorbance at 400 nm observed during the Mon-to-CMon photoconversion is only 30% of that expected for a photobleaching process (see ref 87), (iii) the fluorescence spectra of P^{CMon}_{360} and $P^{monomerizedLIBM}_{360}$ are essentially identical to that of LIBM, indicating that the reduced chromophores remain localized in the binding sites of these species, and (iv) we failed to observe increases in absorbance at 570 nm in CMon over a period of several hours following photoconversion, indicating that BR does not reconstitute, in contrast to bleached PM, which rapidly reconstitutes (see ref 57). The failure of CMon to reconstitute is analogous to that of borohydride-reduced PM, which fails to reconstitute since the chromophore in this species remains covalently bound to the apoprotein (see ref 120). We thus conclude that the chromophore remains covalently bound to the apoprotein in CMon.

generation of LIBM and CMon occurs, and the excitation spectrum of photolyzed CFBM manifests a peak at 466 nm, indicating that $P_{360}^{photolyzedCFBM}$ contains a covalently bound, non-*retro* Schiff base-reduced chromophore with five C=C bonds.

The Nature of P_{605}^{LIBM}. As noted above, the 568→605 nm bathochromic shift resulting from the generation of P_{605}^{LIBM} is similar to those observed when PM is converted to CFBM[24,62−68] and ABM.[1,24,56,62,65,67−71] We thus performed a number of studies to elucidate the relationship of LIBM to CFBM and ABM, the results of which are detailed below.

First, in agreement with Czege and Reinisch,[83] we find that the λ_{max} of LIBM returns to 570 nm upon the addition of cations but that the intensity of the chromophore band is restored to only 30−50% of its original PM value, indicating that ∼50% of the chromophores in LIBM are reduced. The 340, 360, and 380 nm bands are unfaffected by cations, indicating that only the unreduced P_{605}^{LIBM} chromophores shift hypsochromically upon the addition of cations.

Second, in distinct contrast to the bathochromic shift observed during the PM→LIBM photoconversion, the chromophore band shifts *hypsochromically* during the CFBM→photolyzed CFBM photoconversion. The opposite direction of these shifts strongly suggests that the PM→LIBM bathochromic shift is mediated by the removal of Ca^{2+} and Mg^{2+} ions from PM, since CFBM inherently lacks these ions and hence cannot have them photolytically removed.

Third, while we observed essentially identical hypsochromic shifts upon adding equal volumes of 0.0001 *M* Ca^{2+} and 0.01 *M* Na^+ to CFBM, we failed to observe blue→purple transitions in LIBM unless we used concentrated titrants (3.0 *M* Ca^{2+} and 3.0 *M* Na^+). Quantitative comparison of our CFBM and LIBM titrations indicates that Na^+ and Ca^{2+} induce hypsochromic shifts 350 and 13 000 times more efficiently, respectively, in CFBM than in ∼80% LIBM suspensions, and that Ca^{2+} induced hypsochromic shifts only 2−3 times more efficiently than Na^+ in LIBM, in contrast to the 100-fold greater sensitivity to Ca^{2+} in CFBM.[24,66,68,77] (see Table 1). Hence, LIBM binds divalent cations not only more weakly but also less selectively than CFBM. Unfortunately these results do not enable us to specify whether the loss of selectivity results from changes the proximities of pairs of COO^- moieties on BR,[58,62,66] pairs of lipid PO_2^- and SO_3^- moieties,[20,24,77] or combinations of BR COO^- and anionic lipid moieties.[20,77]

Fourth, since the P_{360}^{LIBM} band lies outside the visible range, the blue color of LIBM must originate from BR molecules containing unreduced chromophores. This suggests that the photoreduction of an individual BR molecule induces conformational changes which extend throughout its local environment, resulting in the removal of cations from unreduced BR molecules nearby. As additional support for this conclusion, we find that the magnitude of the Mon→CMon bathochromic shift depends inversely on the ratio of [reduced TX] to [BR], indicating that native lipids play a role in the laser-induced purple→blue color change and suggesting that the bathochromic shift may occur only when micelles are occupied by two or more (at least one reduced and one unreduced) BR molecules.[87] Conformational changes induced by reduced BR molecules cannot account for all of the color change, however, since PM does not turn blue during the early stages of its reduction with borohydride, when only a fraction of the BR molecules present are reduced.[120] Hence, *we believe that the cation removal is mediated by a combination of conformational changes induced by the reduction of BR chromophores plus additional, unspecified laser-induced conformational changes.*

Fifth, the PM→LIBM photoconversion is not mediated by the peroxidation of membrane lipids by $^1O_2$ since LIBM forms in identical fashion in both H_2O and D_2O (data not shown).

In combination, these results indicate that the PM→LIBM bathochromic shift originates from the removal of Ca^{2+} and Mg^{2+} cations from unreduced BR molecules following the photoreduction of the chromophores in ∼50% of the BR molecules in PM. We thus conclude that P_{605}^{LIBM} *consists of unreduced, deionized (CFBM-like) BR molecules which are closely coupled to BR molecules containing non-retro Schiff base-reduced ATRPSB chromophores and that LIBM is generated via the following mechanism:*

PM→LIBM Photoconversion Mechanism.

PM→LIBM Photoconversion Mechanism

$$BR_{570}\,BR_{570}\,BR_{570} \xrightarrow{h\nu_{532}} I^{*}_{460}\,BR_{570}\,BR_{570} \xrightarrow{h\nu_{532}} I^{**}_{460}\,BR_{570}\,BR_{570} \quad \text{(i)}$$

$$I^{**}_{460}\,BR_{570}\,BR_{570} \longrightarrow P_{360}\,BR_{570}\,BR_{570} \quad \text{(ii)}$$

$$P_{360}\,BR_{570}\,BR_{570} \xrightarrow{\text{Conformational changes}}$$

$$P_{360}\,BR_{570}\,BR_{570} \longrightarrow P^{LIBM}_{360}\,BR^{LIBM}_{605}\,BR^{LIBM}_{605} = \text{LIBM} \quad \text{(iii)}$$

$$\downarrow -Ca^{2+} -Mg^{2+} \qquad \downarrow -Ca^{2+} -Mg^{2+}$$

V. Conclusions

On the basis of the studies described above we conclude the following.

(1) Intense 532 nm pulses induce a purple-to-colorless Mon→CMon photoconversion in BR monomers (Mon) solubilized in reduced-TX detergent analogous to the 532 nm-induced purple-to-blue PM→LIBM photoconversion. CMon and LIBM both contain non-*retro* Schiff base-reduced retinyl chromophores in which the C=N bond is reduced to C−N. The reduced chromophores remain covalently bound to the apoprotein in both species. All of the chromophores are reduced in CMon, whereas only ∼50% (1−2 per trimer) are reduced in LIBM.

(2) The rates of the Mon→CMon and PM→LIBM photoconversions both depend quadratically on actinic power and both processes have similar quantum yields, indicating that they are both mediated by a common biphotonic mechanism in which a single BR monomer absorbs two photons.

(3) On the basis of an action spectrum for the PM→LIBM photoconversion obtained in our laboratory, in conjunction with experimental[39,104−106,117] and theoretical [117] $S_1 \rightarrow S_n$ absorption spectra of BR and the temporal characteristics of the laser pulses which effectively generate LIBM,[84,107] we conclude that the excited singlet state I^*_{460} is the intermediate which absorbs the second photon and mediates the generation of LIBM and CMon, with J_{625}, K_{590}, iso-BR, and pseudo-BR playing significantly smaller—if any—roles in the photoconversions. Our data entirely

preclude multi-exciton states, excited states of tryptophan, and short-lived virtual states as intermediates.

(4) The quantum yield for Mon→CMon is roughly twice as large as that for PM→LIBM, indicating that chromophore photoreduction occurs as a result of the absorption of two photons by individual monomers, since $\Phi_{532}^{PM\rightarrow LIBM}$ would greatly exceed $\Phi_{532}^{Mon\rightarrow CMon}$ if multi-exciton intermediates were involved. Furthermore, because the viscosity of PM is 1000 times larger than that of reduced-TX, the quantum yields indicate that significant protein conformational changes do not occur prior to the absorption of the second photon, in agreement with our assignment of I_{460}^{*} as the intermediate.[118]

(5) The blue color of LIBM does not originate from oxidation of membrane lipids by singlet oxygen since LIBM is generated with equal efficiency in H_2O and D_2O.

(6) Metal binding sites are altered during the generation of LIBM as a result of conformational changes induced by the photoreduction of ATRPSB chromophores, leading to the removal of Ca^{2+} and Mg^{2+} ions from binding sites on neighboring native BR monomers.

We are actively pursuing further studies of the PM→LIBM and related photoconversions in our laboratories. These studies should provide additional new insights into the structural and functional roles of BR−BR and BR−lipid interactions in PM, as well as into the potential relationship of these photoconversions to photodegenerative processes in the human retina.

Acknowledgment. We thank Dr. J. A. Stuart and Professors G. R. Allan, S. P. Balashov, R. R. Birge, T. J. Burkey, C. J. Cairns, P. R. Callis, I. V. Chizhov, J. R. Cox, B. Hess, M. Engelhard, and W. Gärtner for helpful discussions, Professor J. G. Stuart, Dr. J. M. McIntyre, A. K. Bunch, B. Buu, J. Chen, T. R. Cullen, G. A. Gerholt, G. L. Gottschalk, M. A. Hammond, J. D. Holland, R. J. Provost, W. C. Spencer, N. E. Sveum, A. L. Trujillo, and Y. Xiao for experimental and editorial assistance, Ms. L. A. Afzali, Mrs. L. Conklin, Ms. E. L. Pyle, Ms. R. G. Raspberry, and Ms. T. Sirls for help with manuscript preparation, Professor J. R. Cox for help with preparation of figures, Professor R. F. Volp for his careful reading of the manuscript, and Professors G. W. Boggess and J. F. Mateja for help procuring intramural and extramural funding. This work was funded by grants from the National Institutes of Health to M.B.M. and D.M.S. (NIH 2S06GM08066-25) and from the National Science Foundation (NSF EPS-9874764), the Research Corporation (C-2974), the Christian Scholars Foundation, and grants-in-aid from Murray State University to M.B.M.

Supporting Information Available: Details regarding (1) deconvolution of the spectra of pure LIBM and CMon from those of PM + LIBM and Mon + CMon mixtures and the physical origin of the small initial Mon-to-CMon bathochromic shift, (2) fluorescence spectra, (3) ΔA_{400} calculations, (4) quantum yields, (5) the PM-to-LIBM action spectrum, and (6) details of our titrations of CFBM and LIBM with metal cations (PDF). This material is available free of charge via the Internet at http://pubs.acs.org.

JA010116A